

Supporting Information

Exploiting Robust Biopolymer Network Binder for Ultrahigh-Areal-Capacity Li-S Battery

Jie Liu,^a Dilini G. D. Galpaya,^b Lijing Yan,^a Minghao Sun,^a Zhan Lin,^{a*} Cheng Yan,^b
Chengdu Liang^a and Shanqing Zhang^{c*}

^a*Key Laboratory of Biomass Chemical Engineering of Ministry of Education, College of Chemical and Biological Engineering, Zhejiang University, Hangzhou 310027, China*

^b*School of Chemistry, Queensland University of Technology, QLD 4001, Australia*

^c*Centre for Clean Environment and Energy, Environmental Futures Research Institute and Griffith School of Environment, Gold Coast Campus, Griffith University, QLD 4222, Australia*

**Corresponding author. zhanlin@zju.edu.cn (Z. Lin), s.zhang@griffith.edu.au (S. Zhang)*

Experimental section

Binder: Guar gum (GG, SARDA, India) and xanthan gum (XG, Aladdin, China) with a mass ratio of 3:1 were stirred in deionized water over night at room temperature to prepare the biopolymer network binder (named as N-GG-XG binder) via the intermolecular binding effect. The strongest interaction between GG and XG in deionized water occurs at the mass fraction of 20-30% for XG,¹ which was used to determine the mass ratio between GG and XG (i.e., 3:1). FTIR spectra were recorded on a FTIR spectrophotometer (Nicolet 5700) in the range of 4000–400 cm⁻¹ using KBr pellets to study the formation of the biopolymer network binder. XRD patterns were also obtained to indicate the change of polymer molecular chain arrangement due to the intermolecular binding effect.

Li-S cell: To prepare the sulfur electrode, sulfur/super P composite, super P conductive carbon, and the N-GG-XG binder with a mass ratio of 8:1:1 were stirred in deionized water to form homogeneous slurry. Sulfur/super P composite was prepared in a sealed Teflon container by simply heating pre-mixed sulfur and super P carbon at a weight ratio of 6:4 for 16 h at 155 °C. The slurry was coated onto current collector via a common doctor-blade coating method. After drying in a vacuum oven at 60 °C over night, the as-prepared electrode was assembled into 2025 coin cell in an Ar-filled glove box using metallic lithium wafer as counter electrode and Celgard 2400 membrane as separator. The electrolyte contained 1 mol L⁻¹ lithium bis(trifluoromethane sulfonyl) imide (LiTFSI) in a binary solvent of 1,3-dioxolane (DOL) and dimethoxyethane (DME) (1:1 in volume) with 1.5 wt% lithium nitrate (LiNO₃) as additive.² The electrolyte/sulfur ratios of high-loading Li-S batteries are around 21.0, 11.5, and 7.8 μL mg⁻¹ for electrodes with sulfur loading of 6.5, 11.9, and 19.8 mg cm⁻², respectively. For comparison, sulfur electrodes with the polyvinylidene fluoride (PVDF, HSV900) binder, gelatin (Sinopharm, China) binder, GG binder, and XG binder were also prepared in the same processes. Deionized water was used as dispersant for gelatin, GG, and XG, and N-methyl-2-pyrrolidone (NMP) for PVDF.

Electrochemical test: To evaluate electrochemical performance, galvanostatic charge-discharge cycling test was carried out at room temperature using LAND battery cycler (China) between 1.5 and 2.8 V. The discharge cut-off voltage of 1.5 V was chosen here due to insulating property of sulfur and large electrochemical polarization in the case of high-loading electrode, though LiNO₃ is irreversibly reduced below 1.7 V.^{3,4} Cyclic voltammetry (CV) study of the electrode was recorded on an electrochemical work station (Solartron 1470E) between 1.5 and 2.8 V at a scan rate of 0.1 mV s⁻¹. All potentials presented in this study were quoted versus the Li/Li⁺ scale.

Mechanical property test: In nano-scratch tests, a conical probe with 5 μm tip radius was used to scratch over the sample surface for obtaining friction coefficient information. During the scratch process, the load was kept constant as 2000 μN and

scratch length was 10 μm . Indentation test was done using the same probe under controlled load with maximum force of 500 μN .

References

- 1 C. Schorsch, C. Gamier and J. L. Doublier, *Carbohydr. Polym.*, 1997, **34**, 165–175.
- 2 S. S. Zhang, *Electrochim. Acta*, 2012, **70**, 344–348.
- 3 S. H. Chung, C. H. Chang and A. Manthiram, *Energy Environ. Sci.*, 2016, **9**, 3188–3200.
- 4 G. Zhou, L. Li, C. Ma, S. Wang, Y. Shi, N. Koratkar, W. Ren, F. Li and H. M. Cheng, *Nano Energy*, 2015, **11**, 356–365.

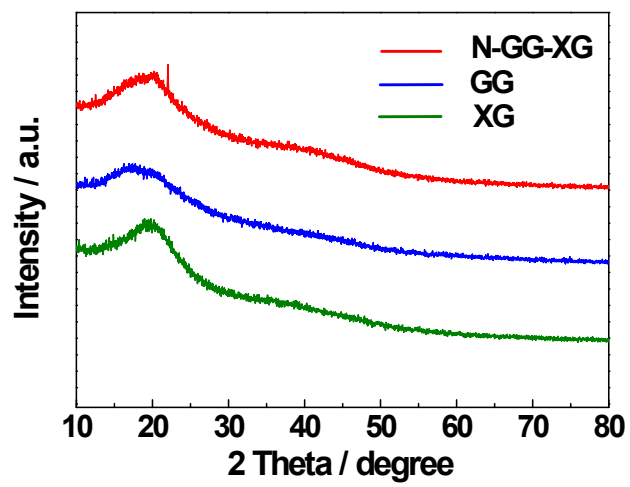


Fig.S1 XRD patterns of GG, XG, and N-GG-XG.

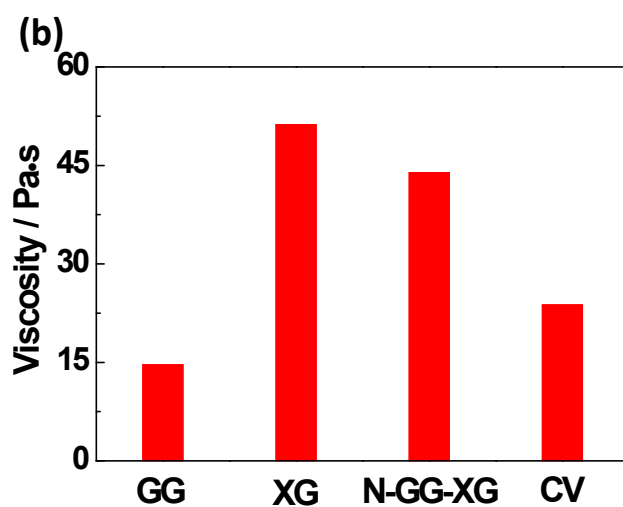
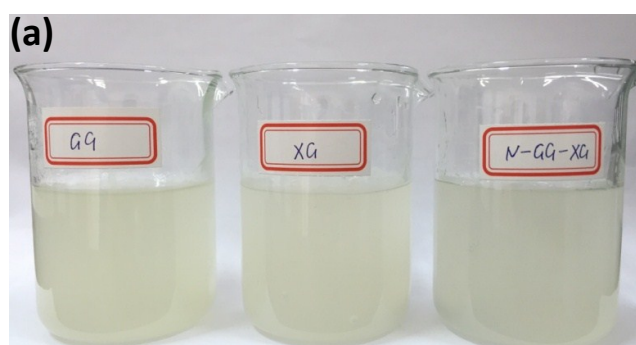


Fig.S2 (a) Photo in solubility of GG, XG, and N-GG-XG confirms water solubility of N-GG-XG; (b) viscosity of GG, XG, and N-GG-XG (1 wt%) at 25 °C. Calculative viscosity (CV) is calculated as the mass ratio of GG and XG in N-GG-XG (3:1).

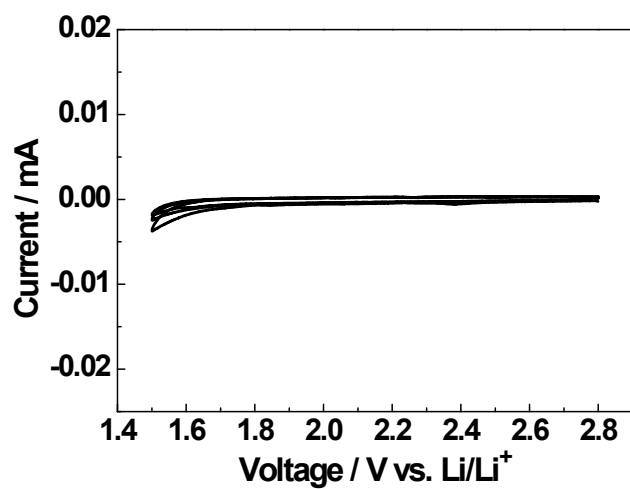


Fig.S3 CV curves of pure N-GG-XG binder at a scan rate of 0.1 mV s^{-1} between 1.5 and 2.8 V. The electrode is composed of the N-GG-XG binder and super P conductive additive with a mass ratio of 1:1. The electrolyte contains 1 mol L^{-1} LiTFSI in a binary solvent of DOL and DME (1:1 in volume).

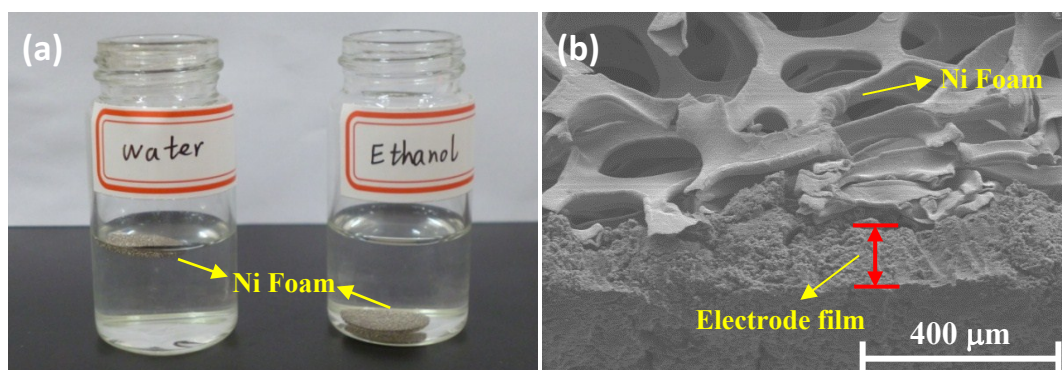


Fig.S4 (a) Photo of Ni foam current collectors in water and ethanol showing the hydrophobicity of Ni foam (even vacuumed using transition chamber of glove box); (b) cross-section SEM image of the S@N-GG-XG electrode showing the thick electrode film on the surface of Ni foam current collector due to the hydrophobicity of Ni foam.

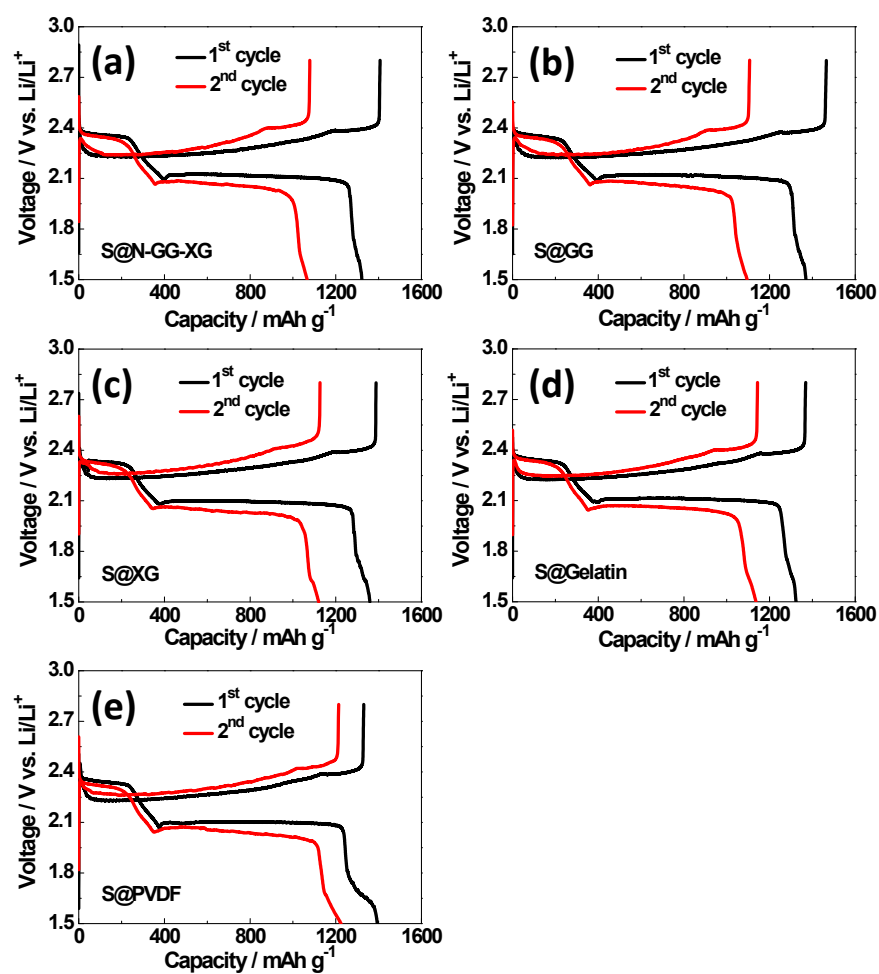


Fig.S5 Charge-discharge curves of the high-loading sulfur electrodes with sulfur loading of 6.5 mg cm⁻² using (a) N-GG-XG, (b) GG, (c) XG, (d) gelatin, and (e) PVDF binders.

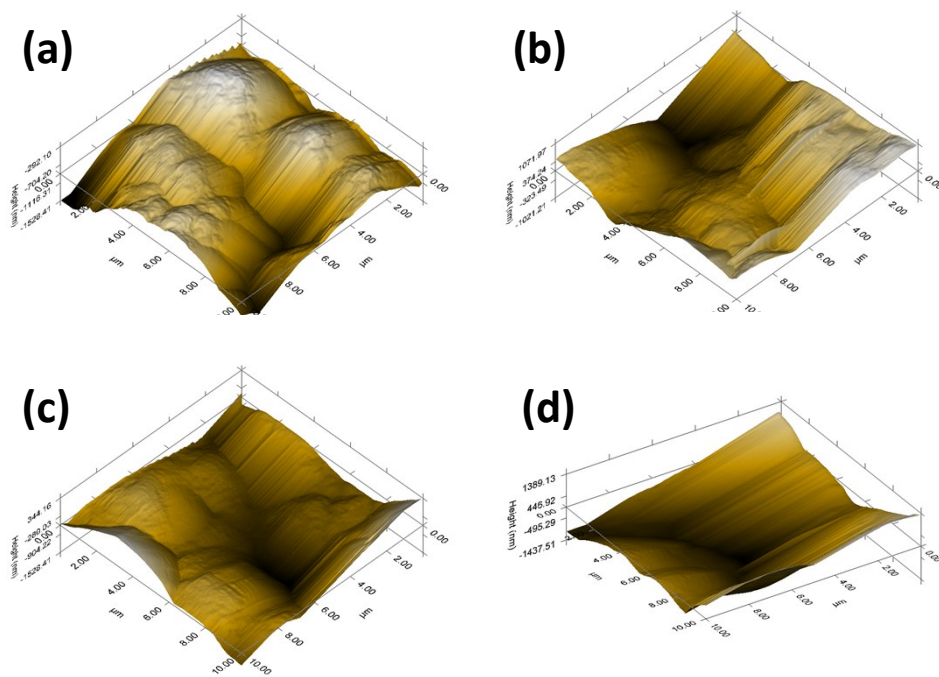


Fig.S6 In situ 3D nano-scratch images of (a) S@GG electrode, (b) S@XG electrode, (c) S@gelatin electrode, and (d) S@PVDF electrode.

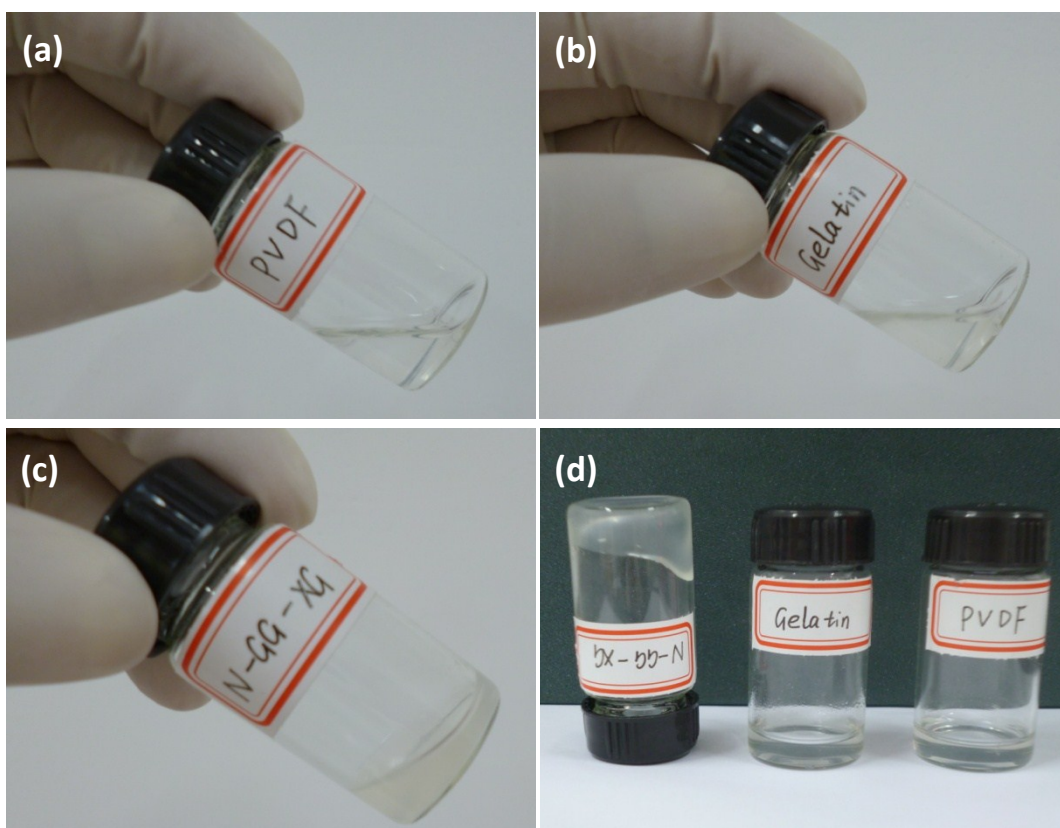


Fig.S7 Photos of (a) PVDF binder, (b) gelatin binder, (c) N-GG-XG binder, and (d) inverted N-GG-XG binder showing the hydrogel property of the N-GG-XG binder.

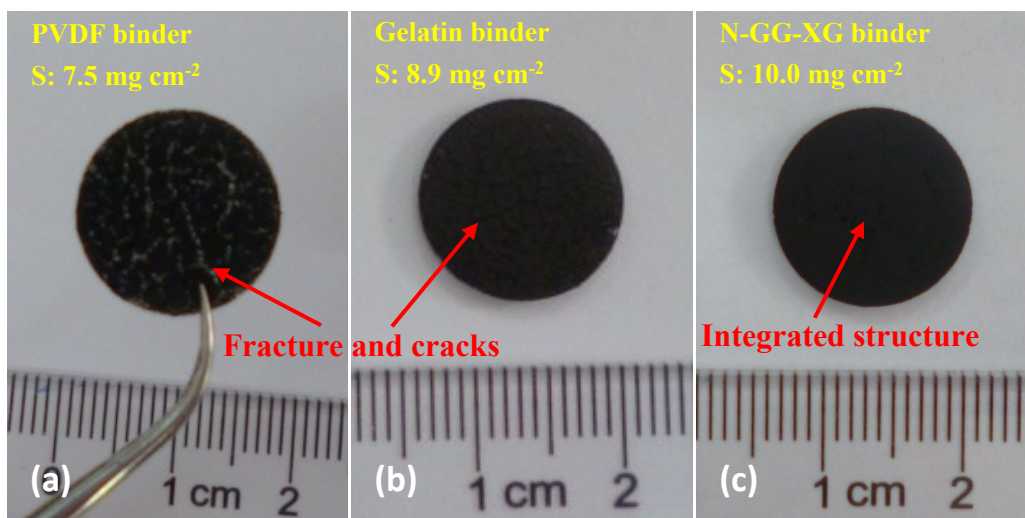


Fig.S8 Photos of (a) S@PVDF electrode, (b) S@gelatin electrode, and (c) S@N-GG-XG electrode showing the integrated electrode structure of the S@N-GG-XG electrode with high sulfur loading owing to the robust mechanical property of the N-GG-XG binder. On the other hand, the S@gelatin electrode and S@PVDF electrode deliver higher capacity than the S@N-GG-XG electrode, which is because that the cracked electrode structures of the S@gelatin electrode and S@PVDF electrode make electrolyte more easily diffuse into the interior of thick electrode.

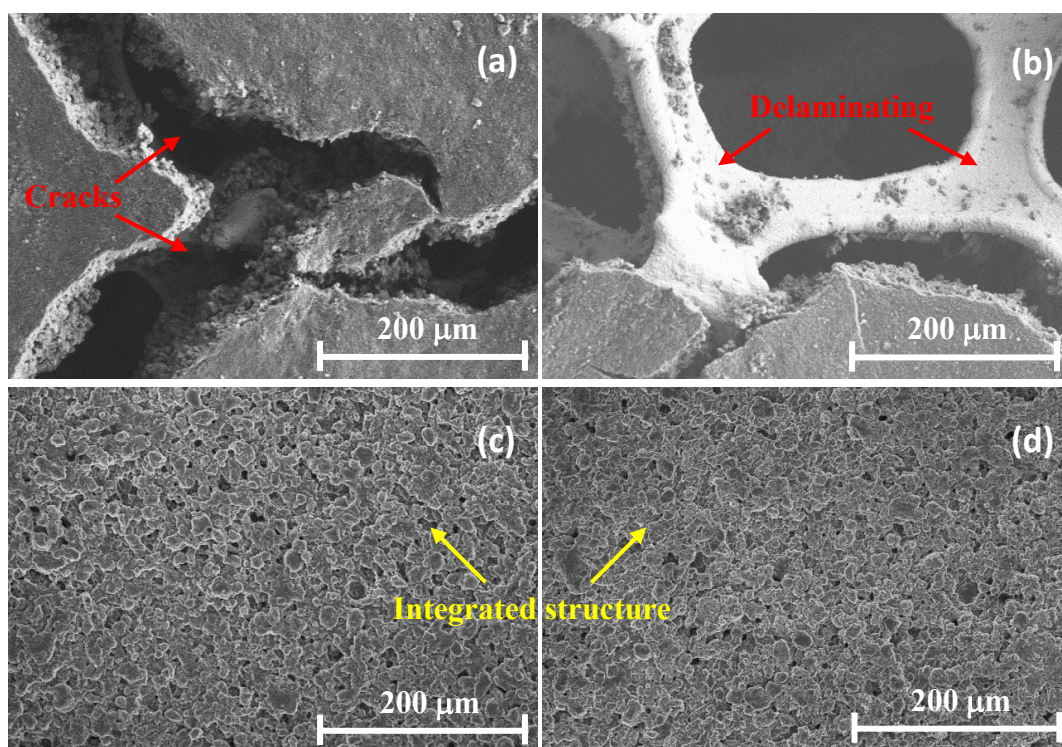


Fig.S9 SEM images of S@gelatin electrodes (a) before cycling and (b) after 30 cycles, and S@N-GG-XG electrodes (c) before cycling and (d) after 30 cycles.

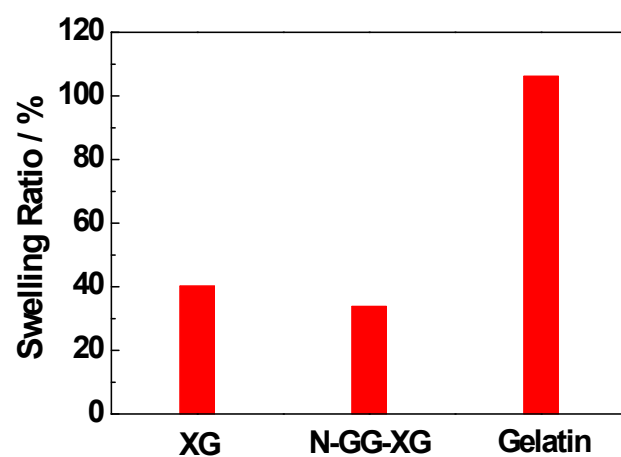


Fig.S10 Swelling property of XG, N-GG-XG, and gelatin binders to exemplify weak swelling property of N-GG-XG binder. Swelling ratio is defined as the weight ratio of the amount of solvent absorbed after soaking binder in the electrolyte for 30 h to the weight of the binder before soaking.

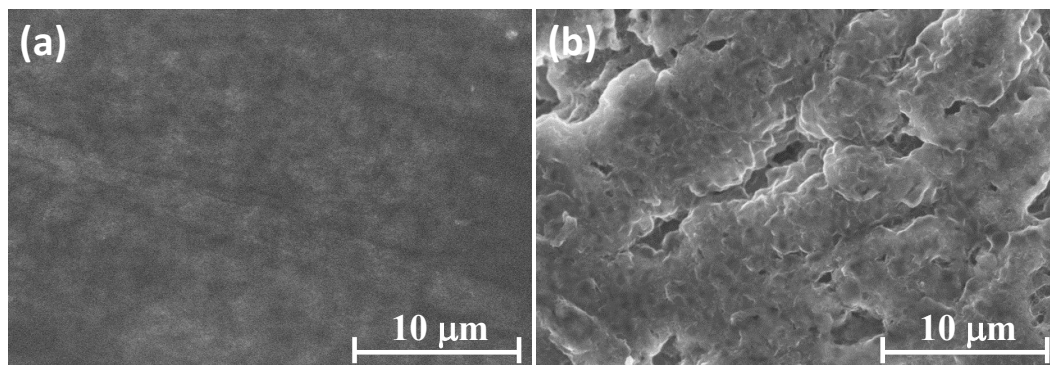


Fig.S11 SEM images of (a) fresh Li anode and (b) Li anode after cycling at 1.6 mA cm⁻² in the Li-S battery using S@N-GG-XG cathode with sulfur loading of 8.8 mg cm⁻².

Table S1 Binder materials in recently published binder-related Li-S batteries in Fig.5b.

reference	binder material
19	gelatin
21	carbonyl- β -cyclodextrin
22	gum arabic
39	PEO:PVP mixture
40	poly(9, 9-dioctylfluorene-co-fluorenone-co-methylbenzoic ester)
41	polyamidoamine dendrimers
42	starch
43	LA132 (a kind of polyacrylonitrile)
44	mixture of polyacrylic acid and poly(3,4-ethylenedioxythiophene):poly(styrenesulfonate)